ELSEVIER

Inorganica Chimica Acta 226 (1994) 137–143

Inorganica Chimica Acta

Solvent, electrolyte and solute shape effects on optical electron transfer in mixed-valence ruthenium ammine dimers

Kent W. Lau, Aron Min-Hom Hu, Michael Hung-Ju Yen, Ella Y. Fung, Stephanie Grzybicki, Regina Matamoros, Jeff C. Curtis *

Chemistry Department, University of San Francisco, 2130 Fulton Street, San Francisco, CA 94117, USA

Received 24 March 1994

Abstract

A series of nine mixed-valence ruthenium ammine dimers have been synthesized and their intervalence transfer spectra have been studied in a group of 14 solvents. The importances of both dielectric continuum effects and specific solvent–solute interactions in defining the nature of the solvent dependences of the IT absorption energies have been addressed. Specific solvent–solute effects predominate for most of the members in the series. Dielectric continuum effects predominate only for the $(NH_3)_5Ru(4,4'\text{-bipyridine})Ru(NH_3)_5{}^{5+}$ system (dimer 7 of the series investigated). Four of the members of the series show evidence for a dual solvent dependence. Ion-atmosphere/ion-pairing effects are at their maximum for dimer 7.

Keywords: Optical electron transfer; Ruthenium complexes; Ammine complexes; Mixed valence complexes; Dinuclear complexes

1. Introduction

We have been interested in understanding the role of specific solvent–solute interactions in defining the nature of the outer-sphere barrier to charge transfer processes in ruthenium ammine and polypyridyl-cyano complexes [1–3]. In one of our previous reports, we showed evidence that specific solvent–solute hydrogen bonding interaction can dominate the solvent effects on optical electron transfer in asymmetric mixed-valence ruthenium dimers where one of the metals in the dimer carries ammine ligands [1]. It was shown that the magnitude of the effect was correlated with the Gutmann donor number (DN) [4] scale of solvent basicities. The origin of the effect was attributed to rearrangements of solvent–solute hydrogen bonds upon a change in redox state at the metal. This form of solvent dependence for intervalence transfer absorption energies represented an interesting contrast to the previously observed solvent effects in similar, though not H bonding capable, mixed-valence dimers [5,6]. The earlier studies had proven beyond doubt that the dielectric continuum theory formulated by Marcus [7] and Hush [8] could correctly predict the form of solvent effects on intervalence transfer energies as long as strong, specific solvent–solute interactions were absent or at least not predominant [9].

An intriguing question remained, however, concerning the nature of the solvent dependence observed for the intervalence transfer (IT) absorption energy in the bis-pentaammineruthenium-4,4′-bipyridine (5+) ion

$$(NH_3)_5Ru^{II}(4,4'\text{-bpy})Ru^{III}(NH_3)_5{}^{5+} \xrightarrow{h\nu} (NH_3)_5Ru^{III}(4,4'\text{-bpy})Ru^{II}(NH_3)_5{}^{5+\,*}$$

Creutz [10] had shown that the solvent dependence of the IT band in this system was well-correlated with the $(1/n^2 - 1/D_s)$ solvent parameter of dielectric continuum theory [1]. This dependence was also observed in a subsequent investigation by Hupp and Meyer [11]. That the IT band of this dimer should respond so clearly to the solvent dielectric properties was puzzling to us in light of our work on the asymmetric dimers [1].

The apparent discrepancy between the above-noted observation and the implication from our own work

---

* Corresponding author.

[1] Here n^2 is the square of the refractive index of the medium and represents the polarizability of the medium at high (optical) frequencies. D_s is the static dielectric constant which represents the polarizability of the medium at low frequencies. See Refs. [7–9].

0020-1693/94/$07.00
SSDI 0020-1693(94)04079-B

Table 1

End groups	Bridging ligands		
	Pyrazine	4-Cyanopyridine	4,4′-Bipyridine
$(NH_3)_5Ru$	1	4	7
trans-py$(NH_3)_4Ru$	2	5	8
2,2′-bpy$(NH_3)_3Ru$	3	6	9

py = pyridine; bpy = 2,2′-bipyridine.

Table 2
Solvents used in this study and relevant solvent parameters

Solvent	$(1/n^2-1/D_s)$[a]	Donor number[b]
(1) Nitromethane (NM)	0.4978	2.7
(2) Nitrobenzene (NB)	0.3851	4.4
(3) Benzonitrile (BN)	0.3885	11.9
(4) 2,4-Pentanedione (PD)	0.4248	12.2[c]
(5) Acetonitrile (AN)	0.5289	14.1
(6) Propylene carbonate (PC)	0.4811	15.1
(7) Acetone (AC)	0.4934	17.0
(8) Formic acid (FACD)	0.5144	19.0
(9) 2-Methoxyethanol (ME)	0.4305	19.7[c]
(10) Ethylene glycol (EG)	0.4579	20.0
(11) Dimethylformamide (DMF)	0.4637	26.6
(12) Dimethylsulfoxide (DMSO)	0.4370	29.8
(13) Formamide (FA)	0.4683	36.0
(14) Hexamethylphosphortriamide (HMPA)	0.4365	38.8

[a] Refractive index n and static dielectric constant D_s taken from Ref. [12].

[b] Donor numbers taken from Refs. [4] and [13].

[c] Donor number values for these two solvents taken from Ref. [14].

that ammine ligands should give rise to a dominant donor number solvent dependence has led us to investigate the solvent dependences of the IT bands in a series of symmetrical dimers. We report here on the observed solvent dependences in the series of dimers as defined in Table 1.

Thus in this numbering scheme, the Creutz–Taube ion will be denoted by **1** and the decaammine 4,4′-bpy-bridged species investigated by Creutz [10] will be denoted by **7**. We have employed a set of 14 fairly diverse solvents spanning a broad range of donor number and $(1/n^2-1/D_s)$ values. These are listed in Table 2. We have also assessed the degree to which ionic strength effects impact optical electron transfer energies in a subset of the dimers shown above.

2. Experimental

The compounds used in this work were synthesized according to the methods outlined in Refs. [1] and [15]. Solvents were purchased from Aldrich or VWR and were dried by passing them over a column of activated alumina prior to use. Dried solvents could be stored under sealed conditions and/or over 3 Å molecular sieves for up to several days, but storage for periods much longer than this were found to introduce irreproducibilities into the measurements. The compounds were characterized by differential pulse polarography using either an IBM EC 225 electrochemical analyzer or a Princeton Applied Research Versastat instrument. Near-IR spectra were recorded using a Perkin-Elmer 330 spectrophotometer and one centimeter pathlength quartz cells. Mixed-valence species were generated in situ from the appropriate II,II dimers using solid $Fe^{III}(2,2'\text{-bpy})_3(PF_6)_3$ as oxidant in 0.1 M as supporting electrolyte (see Ref. [1] for details of the preparations of these reagents). See also Section 5.

2.1. Microanalytical results

(bpy)$(NH_3)_3$Ru(4-cyanopyridine)Ru$(NH_3)_3$(bpy)·H_2O: Calc.: C, 23.68; H, 3.06; N, 12.74. Found: C, 23.77; H, 2.89; N, 12.05%.

(bpy)$(NH_3)_3$Ru(pyrazine)Ru$(NH_3)_3$(bpy)·H_2O: Calc.: C, 22.37; H, 2.66; N, 13.04. Found: C, 22.29; H, 2.92; N, 12.49%.

(py)$(NH_3)_4$Ru(pyrazine)Ru$(NH_3)_4$(py): Calc.: C, 14.53; H, 3.31; N, 14.59. Found: C, 14.68; H, 3.24; N, 13.90%.

(py)$(NH_3)_4$Ru(4,4′-bpy)Ru$(NH_3)_4$(py)·$2H_2O$: Calc.: C, 18.92; H, 3.65; N, 13.30. Found: C, 18.34; H, 3.39; N, 13.09%.

Figures and regressions shown in this paper were generated using Jandel Scientific's SigmaPlot for Windows.

3. Results and discussion

Figs. 1–3 show how the IT band energies for dimers **7**, **8** and **5** respond to the solvent. For dimer **7** the IT band correlates well with the dielectric continuum parameter $(1/n_2-1/D_s)$, while for the other dimers in the series, the predominant solvent effect appears to be the solvent donicity. In Table 3 we summarize the solvent dependences observed for the dimers studied. The coefficient of determination, r^2, obtained for linear regressions of the IT band energy, denoted by E_{op}, versus the single solvent parameters $(1/n^2-1/D_s)$ and donor number (DN) as well as the value obtained using a two-parameter fit according to Eq. (1) are given.

$$E_{op}=a(1/n^2-1/D_s)+b(\mathrm{DN})+c \qquad (1)$$

Comparing the single parameter fits to the two-parameter approach we see that in four cases, dimers **3**, **4**, **7** and **8** there is an improvement in r^2 of 10% or greater for the dual parameter fit. Additionally, the

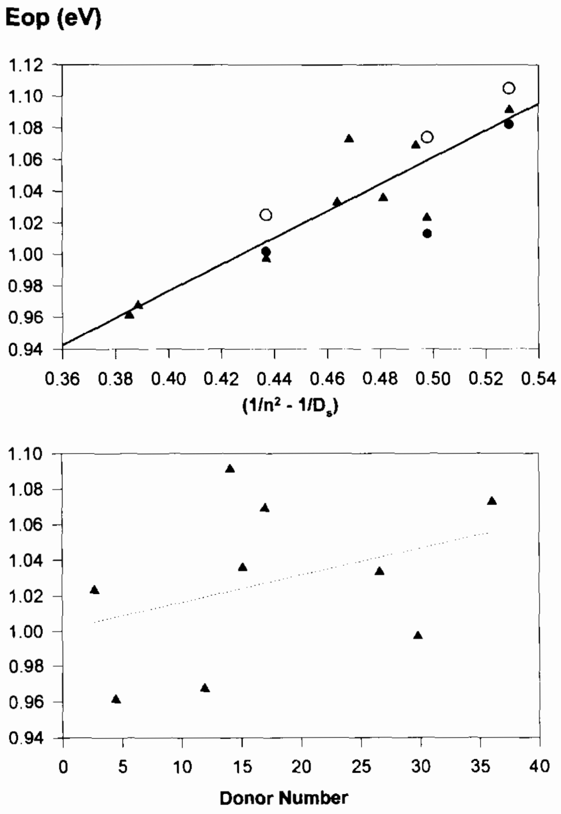

Fig. 1. Energies and solvent correlations observed for optical electron transfer in dimer **7**: ▲, infinite dilution [16]; ●, GP = 0 (this work); ○, GP = 0.256 (this work). The regression line in the upper figure is based on the data from Ref. [16] (filled triangles).

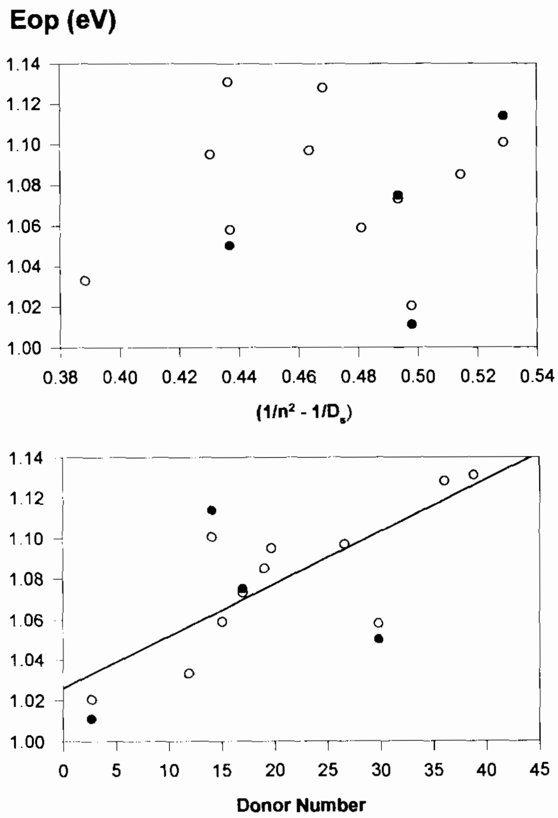

Fig. 2. Energies and solvent correlations observed for optical electron transfer in dimer **8**: ●, GP = 0; ○, GP = 0.256. The regression line in the lower figure is based on the GP = 0.256 data (open circles).

more statistically rigorous extra sum of squares F test [17,18] confirms that these four dimers are indeed exhibiting a statistically meaningful dual solvent parameter dependence at the 90% confidence level. Fig. 4 shows how the correlations appear for the one- and two-parameter solvent fits for the dimer **8**. Only in the case of dimer **9** does there appear to be no significant correlation with either solvent parameter. For the Creutz–Taube ion, dimer **1** in our numbering scheme, our solvent dependence data are in good agreement with the data published recently by Creutz and Chou [19]. Their data yield a slope of 0.00063 eV/DN, an intercept of 0.767 eV and a coefficient of determination of 0.788.

Also listed in Table 3 are the calculated values for the geometric parameter from dielectric continuum theory appropriate to each dimer

$$\xi=\left(\frac{1}{2a_1}+\frac{1}{2a_2}+\frac{1}{d}\right) \qquad (2)$$

where a_1 and a_2 are the hard-sphere radii of the interacting redox sites and d is the distance between them. For symmetric dimers such as the ones studied in this work, a_1 and a_2 are equal (ignoring the radius change due to the change in redox state) and the full Marcus–Hush expression for the dielectric continuum approximation to the outer-sphere reorganizational energy becomes

$$\lambda_0=e_0^2(1/a-1/d)(1/n^2-1/D_s) \qquad (3)$$

where e_0 is the electron charge and the distances are expressed in angstrom units (the resulting energy units for λ_0 are eV/mol if e_0^2 is expressed as 14.4 eV Å/mol). The distances used for the pyrazine, 4-cyanopyridine and 4,4′-bipyridine bridges were 6.8, 9.13 and 11.3 Å, respectively [9,20]. The effective 'sphere of equivalent volume' radii for the $(NH_3)_5Ru$, *trans*-$py(NH_3)_4Ru$ and $(2,2'\text{-bpy})(NH_3)_3Ru$ end groups were calculated to be 3.3, 3.8 and 4.4 Å, respectively, using the method described by Brown and Sutin [21].

3.1. Electrolyte effects

The bulk of the spectroscopic studies reported in this paper were done in solvents containing 0.1 M tetraethylammoniumhexafluorophosphate (TEAH) [14]. This was done in order to retain direct comparability with certain electrochemical experiments that were also being performed. Subsequent to the completion of these experiments, it was pointed out by Lewis and Obeng that even in relatively non-ion pairing electrolytes such as TBAH there could be substantial

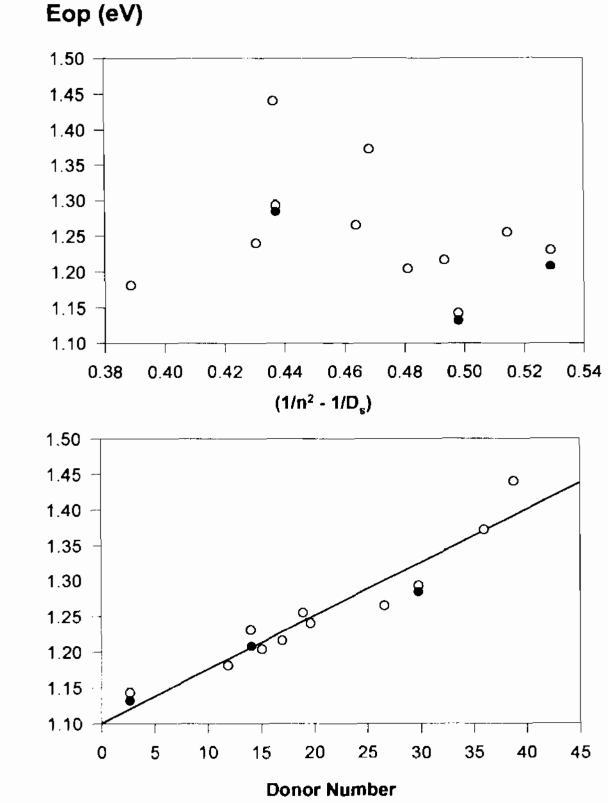

Fig. 3. Energies and solvent correlations observed for optical electron transfer in dimer **5**: ●, GP = 0; ○, GP = 0.256. The regression in the lower figure is based on the GP = 0.256 data (open circles).

spectral shifts induced by ion-pairing and/or ion-atmosphere effects on the IT spectra of dithiaspiroheptane-bridged ruthenium ammine dimers [22]. This effect was also uncovered by Hupp et al. in their studies of the concentration dependence of the IT spectrum dimer **7** [16]. In view of these results, we undertook to determine whether or not ionic strength-related effects were introducing serious uncertainties into the interpretations of our solvent-dependence studies.

Table 4 summarizes the results of the electrolyte effects observed on the systems we have investigated. A parameter often used to correlate ion-atmosphere effects with physical observables such as rates of bimolecular electron transfer [21] or optical electron transfer [22] is the Guggenheim parameter

$$GP = (I^{1/2}/(1+I^{1/2})) \qquad (4)$$

where I is the ionic strength [23]. In Table 4 we list how the optical electron transfer energies vary with GP for the dimers **4**, **5**, **7** and **8** in a variety of solvents. The predicted change in E_{op} derived from the regression lines which would result from a change in GP of 0.000 to 0.256 is also listed. The 0.256 value corresponds to a total ionic strength of 0.118 which is the ionic strength of a solution of 1 mM dimer plus oxidant in 0.1 M TEAH. Also included for reference is the total range in E_{op} spanned for each dimer over the whole set of solvents.

From these data, we see that the spectral shifts induced by ionic strength effects on these systems are clearly measurable, but also small compared to the overall solvent effects. This is also evident upon inspection of Figs. 1–3 where the offset between the zero–GP extrapolated data (filled circles) and the data measured at GP = 0.256 (open circles) is displayed. We note that our zero–GP extrapolated data for dimer **7** are clearly in good agreement with the infinite dilution data for this same dimer reported in Ref. [16] (see Fig. 1, filled triangles).

Interesting comparisons become evident if we consider how the slopes of the E_{op} versus GP plots vary from dimer to dimer. Clearly dimer **7** exhibits a more sensitive dependence on GP than the other species listed in Table 4. Averaging the E_{op} versus GP slopes over all solvents measured for dimers **8**, **4** and **5** yields a mean dependence of 0.017+/−0.033 eV/GP while the average over dimer **7** gives a mean dependence of 0.14+/−0.08 eV/GP. If we evaluate the E_{op} versus GP slope from the data in Ref. [16] over the increment in GP corresponding to 0 ionic strength (same as infinite dilution) and 1 mM dimer plus oxidant (GP = 0.118), we find a very similar mean dependence of 0.13+/−0.17 eV/GP.

Since dimer **7** has the largest ξ value of any dimer in Table 3, it is reasonable to hypothesize that perhaps the same molecular shape parameters that render dimer **7** uniquely sensitive to dielectric continuum effects also render it more sensitive to ion-atmosphere effects. A complicating issue arises, however, if the data published by Lewis and Obeng on the decaamminedithiaspiroheptane system is taken into account. For this dimer, the metal–metal distance is identical to that for dimer **7** at 11.3 Å [25]. Since the end groups are the same, we arrive at an identical ξ value of 0.215. Surprisingly, the observed E_{op} versus GP slope in DMSO with tetrabutylammoniumhexafluorophosphate (TBAH) as electrolyte is 1.07 eV/GP. This is nearly a factor of eight higher than our best estimate for the mean sensitivity of dimer **7**, and it is more than eleven times the sensitivity we observe in DMSO specifically. It seems unlikely that the difference between TEAH and TBAH can account for this variation. Thus it would appear that a given dimer's sensitivity to ion-atmosphere and/or ion-pairing effects probably involves more than simple shape factors alone can predict or explain. It should be noted, however, that subsequent work on the dithiaspiroheptane-bridged species using sodium trifluoroacetate as an electrolyte yields a slope of 0.13 eV/GP in DMSO [24].

An additional complicating factor in the interpretation of ionic strength effects on IT band energies involves the related and additive contributions expected from

Table 3
Single- and two-parameter correlations of E_{op} with solvent

Dimer	ξ[a]	$(1/n^2-1/D_s)$[b]			Donor number			Two parameter[c]		F_{exp}/F_{crit}[f]
		Slope	Intercept	r^2	Slope	Intercept (eV)	r^2	Intercept (eV)	r^2	
1	0.156			0.074	0.000485	0.775	0.794	0.782	0.802	0.16
2	0.116			0.049	0.00011	0.716	0.591	0.684	0.630	0.29
3	0.0802	0.344	0.688	0.163	0.00359	0.786	0.737	0.646	0.867	2.29
4	0.194			0.048	0.00324	1.151	0.735	1.008	0.854[d]	1.29
5	0.154			0.082	0.00783	1.088	0.919	1.090	0.9195	0
6	0.118			0.007	0.00352	1.224	0.609	1.235	0.610	0.023
7	0.215	0.847	0.638	0.810	0.0015	1.001	0.136	0.628	0.890[d,e]	1.29
8	0.175			0.010	0.00258	1.026	0.620	0.875	0.739	1.05
9	0.139			0.042	0.00114	1.194	0.334	1.196	0.336	0.038

[a] See Eq. (2).

[b] See Eq. (3).

[c] See Eq. (1).

[d] Omits data point for hexamethylphosphortriamide.

[e] Data taken from Ref. [16].

[f] F_{exp} values calculated according to the formula $F(p_2-p_1, h-p_2)=((S_1-S_2)(h-p_2))/((p_2-p_1)S_2)$ where p_1 and p_2 are the number of parameters in the single and dual x-parameter fits (2 and 3, respectively), h is the number of points, and S_1 and S_2 are the sums of squares of the residuals for the single and dual x-parameter fits (see Ref. [17]). The F_{crit} values are taken at the 90% confidence level according to Ref. [18].

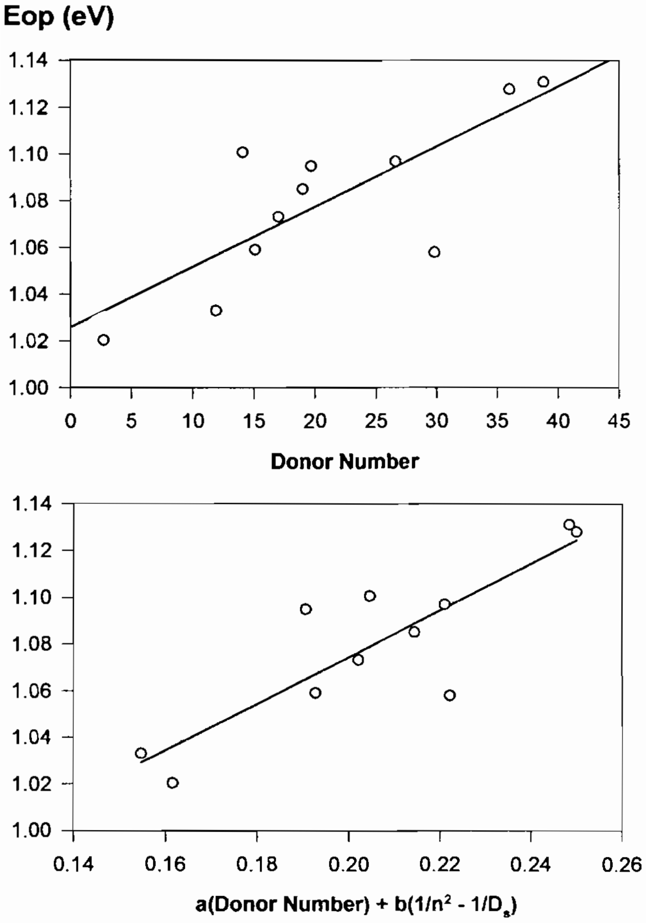

Fig. 4. Illustration of the difference between single (donor number) parameter solvent fit for the data from Fig. 2 (dimer **8**) and the dual parameter fit (Eq. (1)).

both diffuse ion-atmosphere *and* specific ion-pairing effects. Kuznetsov et al. [26] have discussed this issue in depth and raise the notion that the two might be distinguishable on the basis of an expected plateau region for specific ion-pairing interactions where further increases in ionic strength have no effect due to saturation of the relevant ion-pairing equilibrium. This plateau region is evident in the studies of ion-pairing effects on the IT absorption of the biferrocenylacetylene ion which were carried out by Blackbourn and Hupp [27].

We detect what is probably evidence for the roles of both processes in our systems if we compare, for example, the plots of E_{op} versus GP for dimer **7** in nitromethane (NM) and dimer **5** in DMSO. As shown in Fig. 5, the data for dimer **5** in DMSO follow the linear dependence which would be expected for either a pure ion-atmosphere effect or an ion-pairing effect below the point of equilibrium saturation. This is the typical behavior we see. Dimer **7** in NM, however, shows clear evidence of a plateau region and perhaps some additional structure. It is the steeply rising part of this curve which we report as the slope in Table 4. By way of contrast, dimer **9** in NM exhibits a shallow initial slope (reported in Table 4) and some evidence for the onset of a steeply sloping region at GP values in excess of 0.35. That ion-pairing effects might be relatively more important in the lower donor number solvent NM would be in accord with our previous observation that ion-pairing effects between ruthenium(III) ammine fragments and bromide ion appear to be more important in lower-donicity solvents [1]. Presumably the reason lies in the relatively weaker

Table 4
Electrolyte effects of added tetraethylammoniumhexafluorophosphate on intervalence transfer absorption energies

Dimer	Solvent	Slope of E_{op} vs. GP[a] (eV/GP)	ΔE_{op} (GP 0→0.256)[b] (eV)	Total E_{op} range over all solvents[c] (eV)
(7) $A_5(4,4'\text{-bpy})A_5$	NM	0.2470	0.0610	0.130
	AN	0.0900	0.0230	0.130
	DMSO	0.0927	0.0230	0.130
(8) $A_4(4,4'\text{-bpy})A_4$	NM	0.0367	0.0094	0.111
	AN	−0.0510	−0.0130	0.111
	AC	−0.0040	−0.0010	0.111
	DMSO	0.0309	0.0078	0.111
(4) $A_5(4\text{CNpy})A_5$	NM	0.0074	0.0019	0.119
	AN	−0.0167	−0.0043	0.119
	AC	0.0130	0.0033	0.119
	DMSO	0.0628	0.0161	0.119
	HMPA	−0.0107	−0.0027	0.119
(5) $A_4(4\text{CNpy})A_4$	NM	0.0438	0.0110	0.297
	AN	0.0560	0.0143	0.297
	DMSO	0.0582	0.0149	0.297

[a] GP denotes the Guggenheim parameter; GP = $(I^{1/2}/(1+I^{1/2}))$. See text and Refs. [21–24].
[b] Taken from regressions such as the ones shown in Figs. 5 and 6.
[c] From data at GP = 0.256.

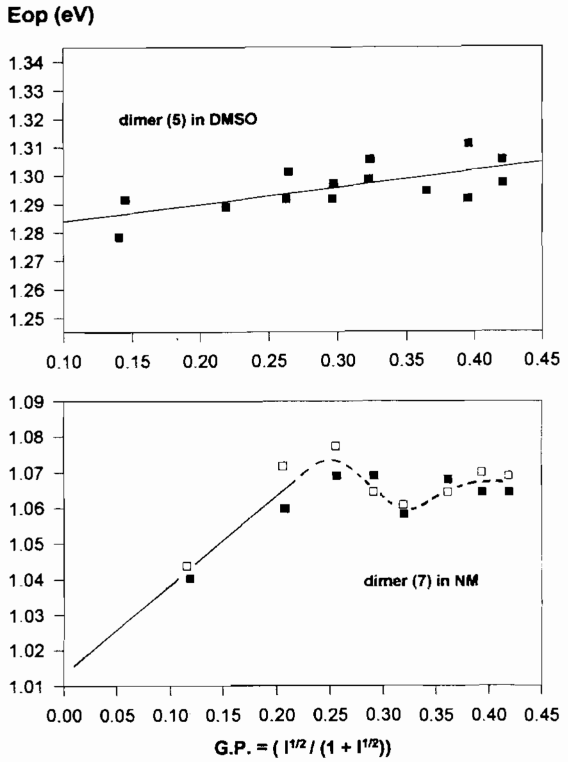

Fig. 5. Ionic strength effects, as indexed by Guggenheim parameter, on the optical electron transfer energies of dimer **5** in DMSO and dimer **7** in NM.

solvent–solute hydrogen bonding interactions in these solvents. Taken together, these results and interpretations would imply that ion-pairing effects, when operative, probably introduce a stronger perturbation to E_{op} than diffuse ion-atmosphere effects (note the large slope for dimer **7** in NM).

4. Conclusions

We note that by far the most sensitive dimer to electrolyte effects appears to be the 4,4′-bipyridine-bridged decaammine species **7** — especially in NM as solvent. This dimer also appears to be unique in that it alone has the familiar dielectric continuum theory-related form [5–9] to its IT solvatochromism. The IT spectra of the other dimers in our study respond predominantly to solvent Lewis basicity as measured by the Gutmann donor number [4]. It is likely that the especially high value of ξ for dimer **7** is at the root of both observations, thus the results are in accord with expectations arising out of the dielectric continuum theory of Marcus and Hush [7–9]. Qualitatively, the high value of ξ for this dimer means that it most nearly adheres to the assumption of well-separated interacting spheres which is central to the derivation of Eq. (2). Finer levels of correlation between the observed solvent and electrolyte behaviors and the magnitude of the ξ parameter, however, are not readily discernable from our results at this point. It is possible that one of the more sophisticated general treatments of the molecular shape-dependence of dielectric continuum effects might be able to better explain the surprisingly abrupt transition from a dielectric continuum-based to a donicity-based IT solvatochromism [28,29].

The existence of dual-parametric solvent dependences such as those exhibited by dimers **3**, **4**, **7** and **8** would be in accord with general expectations and the large body of work showing that dual- and multiparametric scales are needed in order to fully explain and predict most solvent-dependent phenomena [30–32].

The general area of ion-atmosphere and ion-pairing effects on electron transfer processes presents an interesting experimental and theoretical challenge. As in the case of solvent-sorting effects in mixed-solvent systems [2,33] rearrangement of the ion atmosphere about the interacting redox centers and/or transfer of specifically associated ions (or second-sphere complexing agents) between the centers introduces a new, not-necessarily quadratic component into the reaction coordinate defining the electron transfer process [26]. Work currently in progress in our lab [34] is designed to probe into the kinetic consequences of such interactions both in mixed solvents and with the second-sphere compelxing agent lasalocid A anion [35].

5. Supplementary material

Electrochemical data and full spectral data (extinction coefficients and bandwidths in addition to band positions) on the dimers investigated are available from the authors.

Acknowledgements

Early phases of this work were supported by a grant from Research Corporation. Recent efforts have been made possible by a grant from the National Science Foundation RUI program, Grant No. CHE-9200446. The ruthenium used in these studies was provided as a loan from the Johnson Matthey Aesar/Alfa PGM program. We also wish to thank a reviewer for making us aware of Ref. [17].

References

[1] P. Chang, E.Y. Fung and J.C. Curtis, *Inorg. Chem., 25* (1986) 4233–4241.

[2] K.S. Ennix, P.T. MacMahon, R.I. de la Rosa and J.C. Curtis, *Inorg. Chem., 26* (1987) 2660–2666.

[3] E.Y. Fung, A.M. Chua and J.C. Curtis, *Inorg. Chem., 27* (1988) 1294–1296.

[4] V. Gutmann, *The Donor–Acceptor Approach to Molecular Interactions,* Plenum, New York, 1978.

[5] M.J. Powers and T.J. Meyer, *J. Am. Chem. Soc., 102* (1980) 1289–1297.

[6] B.P. Sullivan and T.J. Meyer, *Inorg. Chem., 19* (1980) 752–755.

[7] R.A. Marcus, *J. Chem. Phys., 43* (1965) 679.

[8] (a) N.S. Hush, *Electrochim. Acta, 13* (1968) 1005–1023; (b) G. Allen and N.S. Hush, *Prog. Inorg. Chem., 8* (1967) 357–444.

[9] C. Creutz, *Prog. Inorg. Chem., 30* (1983) 1–73.

[10] C. Creutz, *Inorg. Chem., 17* (1978) 3723–3725.

[11] J.T. Hupp and T.J. Meyer, *Inorg. Chem., 26* (1987) 2332–2334.

[12] I.A. Koppel and V.A. Palm, in N.B. Chapman and J. Shorter (eds.), *Advances in Linear Free Energy Relationships,* Plenum, London, 1972, pp. 254–258.

[13] Y. Marcus, *J. Solution Chem., 13* (1984) 599–624.

[14] K.W. Lau, *Master's Thesis,* University of San Francisco, CA, 1988.

[15] F.S. Salaymeh, S. Berhane, R. Yusof, R.I. de la Rosa, E.Y. Fung, R. Matamoros, K.W. Lau, Q. Zhen, E.M. Kober and J.C. Curtis, *Inorg. Chem., 32* (1993) 3895–3908.

[16] J.T. Hupp, Y. Dong, R.L. Blackbourn and L. Hong, *J. Phys. Chem., 97* (1993) 3278–3282.

[17] J.F. Rusling, *Crit. Rev. Anal. Chem., 21* (1989) 49–81.

[18] N.R. Draper and H. Smith, *Applied Regression Analysis,* Wiley, New York, 2nd edn., 1966.

[19] C. Creutz and M.H. Chou, *Inorg. Chem., 26* (1987) 2995–3000.

[20] D.E. Richardson and H. Taube, *J. Am. Chem. Soc., 105* (1983) 40–51.

[21] G.M. Brown and N. Sutin, *J. Am. Chem. Soc., 101* (1979) 883–892.

[22] N.L. Lewis and Y.S. Obeng, *J. Am. Chem. Soc., 110* (1988) 2306–2307.

[23] E.A. Guggenheim and J.C. Turgen, *Trans. Faraday Soc., 15* (1955) 747.

[24] N.L. Lewis, Y.S. Obeng and W.L. Purcell, *Inorg. Chem., 28* (1989) 3796–3799.

[25] C.A. Stein, N.A. Lewis and G. Seitz, *J. Am. Chem. Soc., 104* (1982) 2596–2599.

[26] A.M. Kuznetsov, D.K. Phelps and M.J. Weaver, *Int. J. Chem. Kinet., 22* (1990) 815–827.

[27] (a) R.L. Blackbourn and J.T. Hupp, *Chem. Phys. Lett., 150* (1988) 399–405; (b) *J. Phys. Chem., 94* (1990) 1788–1793.

[28] R.D. Cannon, *Adv. Inorg. Chem. Radiochem., 21* (1978) 179–230.

[29] B. Brunschwig, S. Erhenson and N. Sutin, *J. Phys. Chem., 90* (1986) 3657–3668.

[30] O.W. Kolling, *J. Phys. Chem., 96* (1992) 1729–1733.

[31] A.P. Abbott and J.F. Rusling, *J. Phys. Chem., 94* (1990) 8910–8912.

[32] A. Tatehata, H. Oota, T. Fukagawa, R.M.L. Warren and A.G. Lappin, *Inorg. Chem., 94* (1993) 8910–8912.

[33] (a) J.T. Hupp and J. Weydert, *Inorg. Chem., 26* (1987) 2657–2659; (b) R.L. Blackbourn and J.T. Hupp, *J. Phys. Chem., 92* (1988) 2817–2820; (c) *Inorg. Chem., 28* (1989) 3786–3790.

[34] (a) Yan Chen, *Master's Thesis,* University of San Francisco, CA, 1992; (b) Qian Zhen, *Master's Thesis,* University of San Francisco, CA, 1993; (c) P. Jamison, W. Mao, R. Foroughi and J.C. Curtis, Work in progress.

[35] J.S. Shaw and G.W. Everett, *Inorg. Chem., 24* (1985) 1917–1920; F. Takusagawa, J. Shaw and G.W. Everett, *Inorg. Chem., 27* (1988) 3107–3112.